Short communication

Li$_2$NaV$_2$(PO$_4$)$_3$: A novel composite cathode material with high ratio of rhombohedral phase

Yuanhao Tang [a], Chenyun Wang [a], Jingjing Zhou [a], Yujing Bi [a], Yang Liu [a], Deyu Wang [a,*], Siqi Shi [b], Guobao Li [c,**]

[a] Ningbo Institute of Material Technology and Engineering, Ningbo, Zhejiang 315201, China
[b] School of Materials Science and Engineering, Shanghai University, Shanghai 200444, China
[c] Beijing National Laboratory for Molecular Sciences, State Key Laboratory of Rare Earth Materials Chemistry and Applications, College of Chemistry and Molecular Engineering, Peking University, Beijing 100871, China

G R A P H I C A L   A B S T R A C T
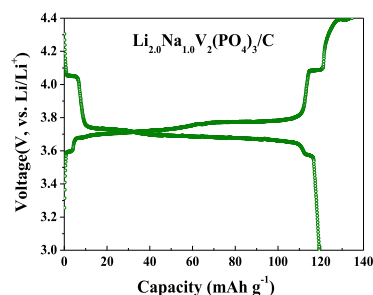
A R T I C L E   I N F O

A B S T R A C T

A novel composite material Li$_2$NaV$_2$(PO$_4$)$_3$/C is developed by utilizing our latest finding to form less stable rhombohedral Li$_3$V$_2$(PO$_4$)$_3$ directly with partial substitution of Li$^+$ to Na$^+$ ions. In the prepared sample, rhombohedral Li$_3$V$_2$(PO$_4$)$_3$ becomes the dominant phase with a proportion of ∼59%, coexistent with monoclinic Li$_3$V$_2$(PO$_4$)$_3$ (10%) and rhombohedral Na$_3$V$_2$(PO$_4$)$_3$ (31%). High-resolution transmission electron microscopy (HRTEM) reveals that different phases coexist in the same primary particles. This characteristic is different from other cathodes, in which the primary particles are single- or poly-crystals. The prepared composite delivers a discharge capacity of 119.1 mAh g^{-1}, of which 93.6% is centralized around 3.7 V vs. Li/Li$^+$, in good agreement with phase's ratio calculated from refinement. The plateaus of monoclinic Li$_3$V$_2$(PO$_4$)$_3$, appeared at 3.6 and 4.1 V vs. Li/Li$^+$, play an additional role of indicator to warn the end of charge and discharge. This kind of electrode materials are particular suitable to build large batteries to power electric vehicles and shape the grid.

1. Introduction

Recently, phosphate cathodes have been gaining the enormous attention due to their advantages on safety and cyclic stability. These characteristics were particularly feasible to construct large batteries potentially used to power electric vehicles and shape the grid. Olivine phosphates, especially LiFePO$_4$ that is firstly proposed by Goodenough et al. [1–3] and revolutionary improved by carbon coating [4,5], have penetrated the market of the aforementioned applications. Various leading companies have invested tremendous resources and mental power to accelerate the industrial development of these materials.

NASICON (Na$^+$ super-ionic conductor) phosphates were another promising cathode owing to the higher Li$^+$ ion mobility, reasonable

capacities and better activity at lower temperature, when compared with olivine LiFePO$_4$. In most cases, monoclinic Li$_3$V$_2$(PO$_4$)$_3$ (Mono-LVP) patented by Valence [6], was recognized as the only representative of NASICON phosphate [7,8]. Li$^+$ ions could be removed at the redox potentials of 3.65, 3.7, 4.1 and 4.8 V vs. Li$^+$/Li corresponding to the extraction of the first half, the second half, the 2nd and 3rd Li$^+$ ions. Restricted by the stability of state-of-art electrolyte, the 3rd Li$^+$ ion was difficult to utilize in practical devices, namely the usable capacity is ca. 131 mAh g^{-1} in theory [9–11].

Rhombohedral structure was the other existent phase of lithium vanadium phosphate. Two cations could be reversibly removed with a redox potential of ~3.7 V vs. Li/Li$^+$ instead of the multi-plateaus of Mono-LVP [12]. However, rhombohedral Li$_3$V$_2$(PO$_4$)$_3$ (Rhom-LVP) could not be synthesized directly since its stability is poorer than that of Mono-LVP [13]. Rhombohedral Li$_2$NaV$_3$(PO$_4$)$_3$ was firstly prepared by Goodenough et al. [14,15] via chemical ion exchange reaction from rhombohedral Na$_3$V$_2$(PO$_4$)$_3$ (Rhom-NVP). In the followed investigations [16], the same method was also used to obtain Rhom-LVP.

In recent efforts, our group found that Rhom-LVP could be produced directly via a simple solid−state reaction when Na$^+$ ions were partially substituted for Li$^+$ ions. The Rhom-NVP phase seemed to work as the inducer to facilitates the generation of rhombohedral Li$_3$V$_2$(PO$_4$)$_3$.

In this paper, it will be introduced the characteristics of a novel composite cathode Li$_2$NaV$_2$(PO$_4$)$_3$/C developed by utilizing the aforementioned mechanism. The prepared material comprises of Rhom-LVP, Mono-LVP and Rhom-NVP, which are coexistent with a ratio of 59:10:31. According to discharge capacity, ~91.4% is contributed from rhombohedral phase. The plateaus of Mono-LVP at 3.6 and 4.1 V vs. Li/Li$^+$ are remained in the charge−discharge curves to play an additional role of indicator of state-of-charge and depth-of-discharge.

2. Experimental

The Li$_2$NaV$_2$(PO$_4$)$_3$ composite were prepared via solid−state reactions. A mixture of LiF (A.R.), NaF (A.R.), NH$_4$VO$_3$ (A.R.), and NH$_4$H$_2$PO$_4$ (A.R.) in stoichiometric molar ratio were ground and mixed together with 10 wt% carbon (Sucrose was acted as carbon source) by ball milling for 4 h. The mass ratio of ball to powder was 5:1 and the rotation speed was 580 rpm. After alcohol was completely evaporated at 60 °C, the precursor was collected and pre-sintered at 400 °C for 4 h and subsequently sintered at 800 °C for 12 h, then cooled down to room temperature under Ar−H$_2$(92:8, v/v) gas atmosphere in a tube furnace. The samples of Li$_3$V$_2$(PO$_4$)$_3$/C and Na$_3$V$_2$(PO$_4$)$_3$/C were synthesized through a similar processing procedure. The material of 2Li$_3$V$_2$(PO$_4$)$_3$·Na$_3$V$_2$(PO$_4$)$_3$/C was obtained via mixing the prepared Li$_3$V$_2$(PO$_4$)$_3$/C and Na$_3$V$_2$(PO$_4$)$_3$/C in molar ratio of 2:1 by ball-milling for 4 h.

The electrode composite was comprised of 80 wt% Li$_{3-x-}$Na$_x$V$_2$(PO$_4$)$_3$/C, 10 wt% super P and 10 wt% polyvinylidene fluoride dissolved in N-methylpyrrolidone. The slurry of electrode composite was coated on aluminum foil current collectors after mixed 2 h. After drying at 120 °C under vacuum, the electrodes were punched into φ16 mm disks. Then, 2032 coin cells were assembled using Celgared 2340TM as the separator, lithium foil as anode, and 1 mol L^{-1} LiPF$_6$ in a mixture solution of EC, DMC and DEC (1:1:1, v/v) as electrolyte. The assembly of the test cells was performed in M-Braun glove box filled with pure argon to keep water and oxygen content less than 1 ppm.

The capacity measurements were performed under a PC-controlled battery tester of Land 2001A (Wuhan, China). The cells were tested at various rates (1 C = 130 mAh g^{-1}) between 3.0 and 4.4 V vs. Li/Li$^+$ at room temperature. The electrochemical capacity

of the samples was calculated based on the amount of the active material excluding the coated carbon. To compare the capacitive ratio, the capacity of monoclinic phase was set as 2 times of the capacity in 4.1 V plateau, and the Rhom-phase's capacity was calculated as the capacity in 3.7 V plateau subtracting half of the capacity in 4.1 V plateau.

The structure and composition of the samples were characterized by X-ray diffraction with a Bruker D8 Advanced diffractometer using CuKα(λ = 1.5406Å) radiation (Bruker AXS, D8 Advance). Morphology was observed with scanning electron microscopy (SEM, HitachiS-4800) and the carbon content was analyzed by PerkinElmer 2400II CHNS/O. The Rietveld refinement were carried out by the GSAS program (Larson and Von Dreele, 2000) via the EXPGUI interface (Toby, 2001) [17,18], and the refinement starting model was chosen on the basis of the monoclinic Li$_3$V$_2$(PO$_4$)$_3$, rhombohedral Li$_3$Fe$_2$(PO$_4$)$_3$ and rhombohedral Na$_3$Fe$_2$(PO$_4$)$_3$ compound from the precedent literature. Microstructure was examined by (SEM) transmission electron microscopy (TEM) on a FEI Tecnai F20 equipped with a field emission gun at an accelerating voltage of 200 kV.

3. Results and discussions

The synthesized Li$_2$NaV$_2$(PO$_4$)$_3$/C is a tri-phase composite instead of the mixture of Rhom-NVP and Mono-LVP, as shown in Fig. 1. A new material, rhombohedral Li$_3$V$_2$(PO$_4$)$_3$, is identified in the
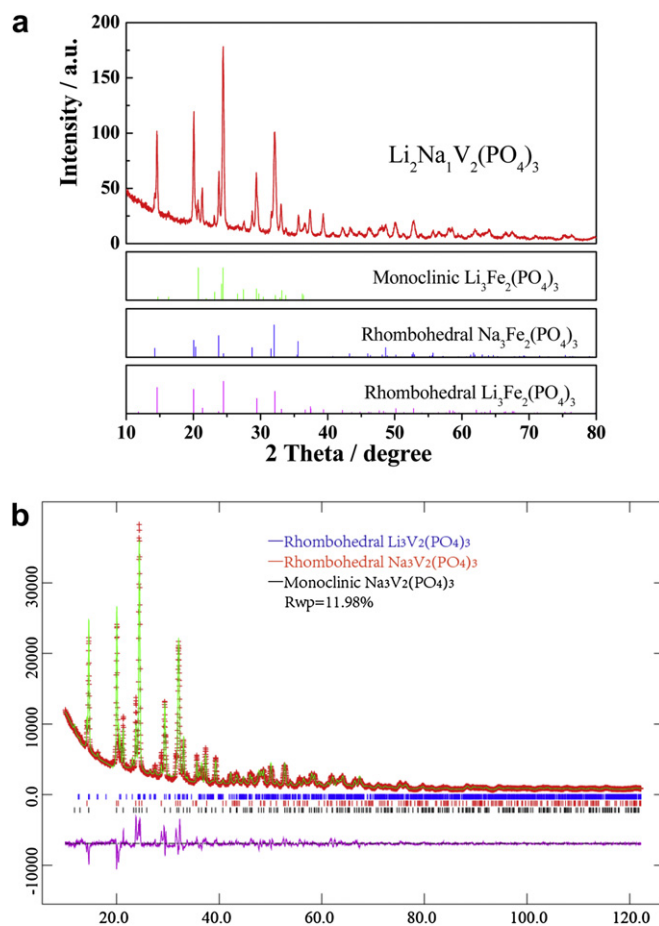
Fig. 1. (a) XRD patterns of Li$_2$NaV$_2$(PO$_4$)$_3$/C, and the comparison with JCPDS of monoclinic Li$_3$Fe$_2$(PO$_4$)$_3$(P2$_1$/n, 47−0107), Rhombohedral Na$_3$Fe$_2$(PO$_4$)$_3$(R-3c, 70-3613) and Rhombohedral Li$_3$Fe$_2$(PO$_4$)$_3$(R-3, 70-3614). (b) XRD profile of the Rietveld refinement for Li$_2$Na$_1$V$_2$(PO$_4$)$_3$/C.

Table 1
Rietveld refinement results of components contained in Li$_2$Na$_1$V$_2$(PO$_4$)$_3$/C.

Materials	Unit cell parameters				Ref.
	a (Å)	b (Å)	c (Å)	V (Å^3)	
Monoclinic Li$_3$V$_2$(PO$_4$)$_3$	8.591	12.038	8.605	889.867	[19]
Rhombohedral Li$_3$Fe$_2$(PO$_4$)$_3$	8.3009	8.3009	22.502	1342.77	[20]
Rhombohedral Na$_3$Fe$_2$(PO$_4$)$_3$	8.7270	8.7270	21.8078	1438.38	[12]
Monoclinic LVP in Li$_2$Na$_1$V$_2$(PO$_4$)$_3$/C	8.6029	12.0414	8.6031	891.147	Present work
Rhombohedral LVP in Li$_2$Na$_1$V$_2$(PO$_4$)$_3$/C	8.3385	8.3385	22.4253	1350.332	Present work
Rhombohedral NVP in Li$_2$Na$_1$V$_2$(PO$_4$)$_3$/C	8.7215	8.7215	21.8516	1439.447	Present work

final product. It is the first time to propose that rhombohedral Li$_3$V$_2$(PO$_4$)$_3$ could be synthesized directly in our best knowledge. According to refinement calculation, the mole ratio of Mono-LVP, Rhom-LVP, and Rhom-NVP is 10:59:31, and their lattice

parameters are in good agreement with those of the reference, as listed in Table 1 [12,19,20]. The slight variance of lattice information between the present work and the references should be resulted from the difference of transitional metals.

The particles of the prepared sample are evenly distributed with a size of ∼200 nm as shown in Fig. 2a. The floccule stuff in the viewing field is the carbon (7.87 wt%) pyrolyzed from sucrose. The microstructure of Li$_2$NaV$_2$(PO$_4$)$_3$/C was analyzed with HRTEM. As shown in Fig. 2b and d, besides the single-phase region (Fig. 2d), the two-phase boundary (Fig. 2c) is clearly identified in the selected particle. The observed planes in Fig. 2c are spaced as 6.193 Å, which is well matched to that of (012) in Rhom-NVP (6.21 Å), and as 6.058 Å, which is possibly attributed to that of (012) in Rhom-LVP (6.062 Å) or (020) in Mono-LVP (6.020 Å). The characteristic of two-phase coexistence is also verified in other particles, as shown in Fig. 2e. The plane with a distance of 6.211 Å could be ascribed to (012) plane of Rhom-NVP, and the second plane (d = 4.236 Å) is
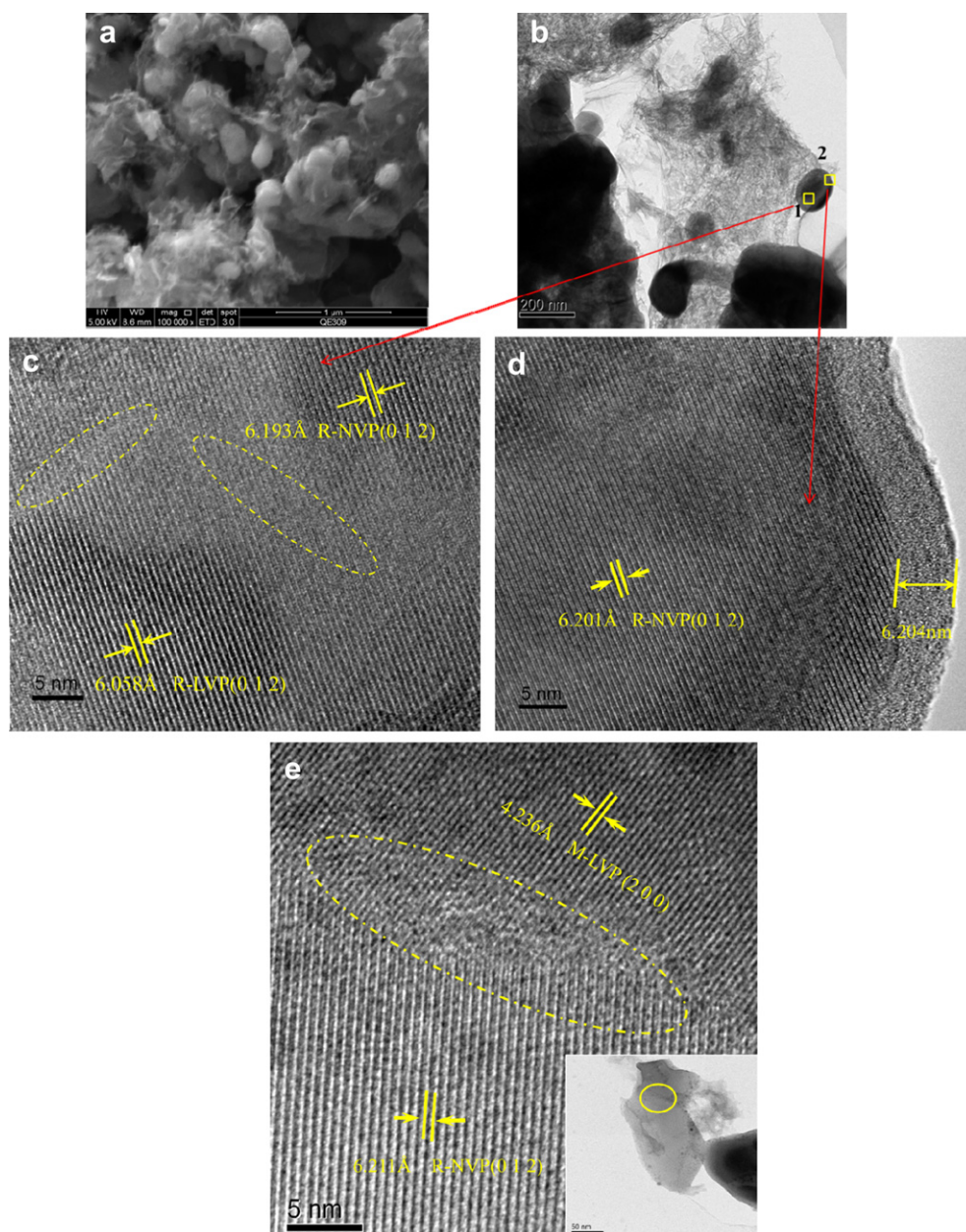
Fig. 2. (a) SEM image of Li$_{2.0}$NaV$_2$(PO$_4$)$_3$/C, (b) TEM picture of Li$_{2.0}$NaV$_2$(PO$_4$)$_3$/C and (c), (d), (e)HR-TEM of selected regions.
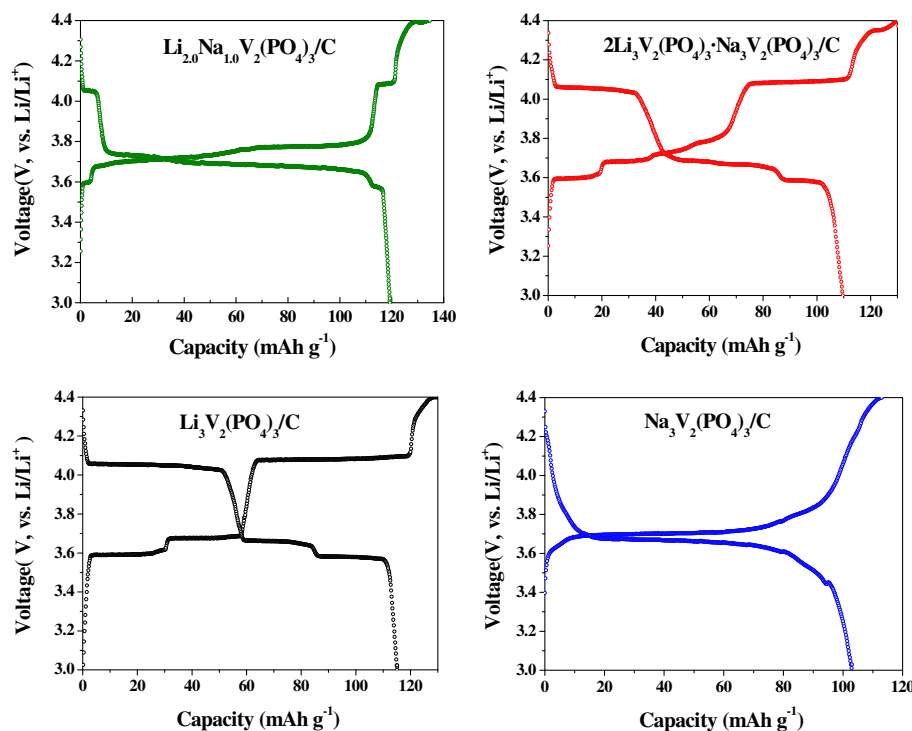
Fig. 3. The 1st charge—discharge curves of $Li_2NaV_2(PO_4)_3$/C, $2Li_3V_2(PO_4)_3 \cdot Na_3V_2(PO_4)_3$/C, $Na_3V_2(PO_4)_3$/C, and $Li_3V_2(PO_4)_3$/C tested at 0.05 C between 3.0 and 4.4 V.

corresponding to that of (002) in Mono-LVP (4.281 Å) or (110) in Rhom-LVP (4.158 Å). As most of d-values between Rhom-LVP and Mono-LVP are very close, the attribution of second plane is still dubious even after various particles were analyzed. It is inclined to ascribe the second phase in Fig. 2c and e to Rhom-LVP and Mono-LVP respectively according to the degree of compatibility. HRTEM results disclose that the microstructure of our sample is different from other crystalline cathodes where the primary particles are single- or poly-crystals. It is worthy to note that the width of phase boundary is 2—4 nm, which is much closer than that of the common mixtures.

The prepared $Li_2NaV_2(PO_4)_3$/C was evaluated electrochemically between 3.0 and 4.4 V $vs.$ Li/Li$^+$. This material presents a reversible capacity of 119.1 mAh g^{-1} as shown in Fig. 3. The capacity centralized at $ca.$ 3.7 V $vs.$ Li/Li$^+$ is 93.6%, including the reaction of rhombohedral phase and the second half in Mono-LVP. The short plat at 3.65 and 4.1 V $vs.$ Li/Li is corresponding to the reversible reaction of the first half and second Li$^+$ ion in monoclinic phase, which could work as the indicator of charge and discharge. Calculated from discharge capacity, the ratio of rhombohedral and monoclinic phase is 91.4:8.6, basically consistent with the phase ratio obtained from refinement. The charge—discharge curves of $2Li_3V_2(PO_4)_3 \cdot Na_3V_2(PO_4)_3$/C, $Na_3V_2(PO_4)_3$/C and $Li_3V_2(PO_4)_3$/C are also compared in Fig. 3 as a control. The reversible capacity of $Li_2NaV_2(PO_4)_3$/C composite is slightly higher than those of $Li_3V_2(PO_4)_3$/C (114.6 mAh g^{-1}), $2Li_3V_2(PO_4)_3 \cdot Na_3V_2(PO_4)_3$/C (109.8 mAh g^{-1}) and $Na_3V_2(PO_4)_3$/C (103.5 mAh g^{-1}). Furthermore, the capacity contributed from rhombohedral phase in $2Li_3V_2(PO_4)_3 \cdot Na_3V_2(PO_4)_3$/C is around 31% of total capacity, which is in good agreement with the phase's proportion. This result proves that rhombohedral $Li_3V_2(PO_4)_3$ is formed directly by partial substitution of Li$^+$ to Na$^+$ in the view of electrochemistry.

The prepared composite presents an excellent rate-capability as shown in Fig. 4. This material delivers a capacity of 105 and

95 mAh g^{-1} at 5 C and 10 C respectively, which is 89% and 81% of discharge capacity at 0.05 C. Similar to other phosphate cathodes, it also exhibits a good cyclic stability, as shown in the inset of Fig. 4. After 100 cycles, the discharge capacity keeps 96.7% and 92.8% cycled at 0.1 C/0.1 C and 1 C/1 C between 3.0 and 4.4 V $vs.$ Li/Li$^+$, respectively.

The electrochemical results demonstrates that our $Li_2NaV_2(PO_4)_3$/C composite possesses a good kinetic capability. This characteristic probably roots in the small crystal domain reduced by multi-phase coexisting in one primary particle with a size of 200 nm. Also the opener structure of rhombohedral phase probably exerts a beneficial influence on Li$^+$ diffusion.
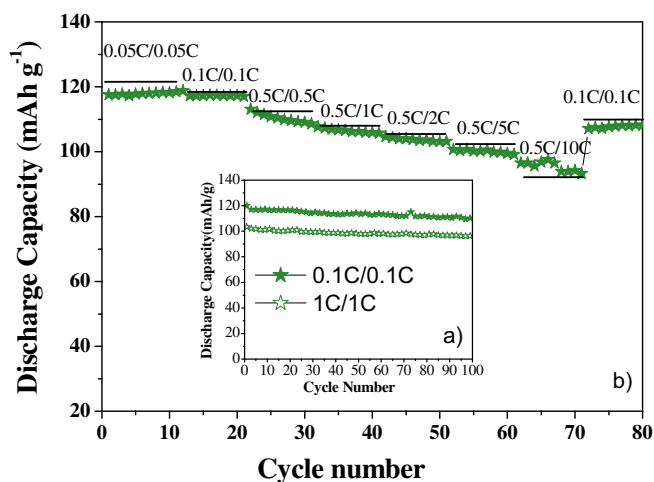

Fig. 4. Rate capability of $Li_2NaV_2(PO_4)_3$/C at various C-rate varied from 0.05 C to 10 C (1 C = 130 mA g^{-1}) between 3.0 and 4.4 V. Inset means the cyclic behavior of the $Li_2NaV_2(PO_4)_3$/C tested at 0.1 C/0.1 C and 1 C/1 C between 3.0 and 4.4 V.

4. Conclusion

Less stable rhombohedral $Li_3V_2(PO_4)_3$ phase has been achieved when part of Li^+ ions were replaced by Na^+ ions. The composite material of $Li_2NaV_2(PO_4)_3$/C was composed of monoclinic $Li_3V_2(PO_4)_3$, rhombohedral $Li_3V_2(PO_4)_3$ and rhombohedral $Na_3V_2(PO_4)_3$ with a mole ratio of 10:59:31. Owing to the phase's proportion, the discharge capacity was mainly contributed from rhombohedral phase, and the short plateaus of Mono-LVP could work as an indicator of the end of charge and discharge. Our discovery of the phenomenon akin to structural inducing effect should provide a new strain of thought to design novel cathode materials utilized in lithium ion batteries.

Acknowledgments

References

[1] A.K. Padhi, K.S. Nanjundaswamy, J.B. Goodenough, J. Electrochem. Soc. 144 (1997) 1188—1194.
[2] A.K. Padhi, K.S. Nanjundaswamy, S. Okada, J.B. Goodenough, J. Electrochem. Soc. 144 (1997) 1609—1613.
[3] J.B. Goodenough, K.P. Akshaya, K.S. Nanjundaswamy, C. Masquelier, US 5910382, 1999.
[4] N. Ravet, J.B. Goodenough, S. Besner, M. Armand, 196th Meeting of the Electrochemical Society Hawaii, USA, 127, 1999.
[5] N. Ravet, Y. Chouinard, J.F. Magnan, S. Besner, M. Gauthier, M. Armand, J. Power Sources 97 (2001) 503—507.
[6] J. Barker, Y. Saidi, US 5871866, 1999.
[7] M.Y. Saïdi, J. Barker, H. Huang, J.L. Swoyer, G. Adamson, Electrochem. Solid State Lett. 5 (2002) A149—A151.
[8] J. Barker, M.Y. Saïdi, S.L. Swoyer, Electrochem. Solid State Lett. 6 (2003) A53—A55.
[9] H. Huang, S.C. Yin, T. Kerr, L.F. Nazar, Adv. Mater. 14 (2002) 1525—1528.
[10] M.M. Ren, Z. Zhou, X.P. Gao, W.X. Peng, J.P. Wei, J. Phys. Chem. C 112 (2008) 5689—5693.
[11] Y.Q. Qiao, J.P. Tu, Y.J. Mai, J.Y. Xiang, X.L. Wang, C.D. Gu, J. Alloys Compd. 509 (2011) 7181—7185.
[12] J. Gaubicher, G. Goward, C. Wurm, C. Masquelier, L.F. Nazar, Chem. Mater. 12 (2000) 3240—3242.
[13] C. Masquelier, C. Wurm, J. Rodriguez-Carvajal, J. Gaubicher, L. Nazar, Chem. Mater. 12 (2000) 525—532.
[14] B.L. Cushing, J.B. Goodenough, J. Solid State Chem. 162 (2001) 176—181.
[15] M. Armand, J.B. Goodenough, A.K. Padhi, K.S. Nanjundaswamy, C. Masquelier, US 5910382, 2003.
[16] C.M. Burba, R. Frech, Solid State Ionics 177 (2007) 3445—3454.
[17] A.C. Larson, R.B. Von Dreele, Los Alamos National Laboratory Report, LAUR, 2004, pp. 86—748.
[18] B.H. Toby, J. Appl. Crystallogr. 34 (2001) 210—213.
[19] S. Patoux, C. Wurm, M. Morcrette, G. Rousse, C. Masquelier, J. Power Sources 119 (2003) 278—284.
[20] P. Eyob, A.S. Andersson, J.O. Thomas, Mater. Chem. 12 (2002) 2343—2347.